55. PRELIMINARY REPORT ON THE PALEOMAGNETISM OF APTIAN AND ALBIAN LIMESTONES AND TRACHYTES FROM THE MID-PACIFIC MOUNTAINS AND HESS RISE, DEEP SEA DRILLING PROJECT LEG 62[1]

William O. Sayre,[2] Oceanography Department, University of Southampton, Southampton, SO9 5NH England

ABSTRACT

Paleomagnetic results are described from Aptian–Albian limestones from Deep Sea Drilling Project Hole 463, on the Mid-Pacific Mountains, and late Albian limestones and a trachyte sequence from Hole 465A, on Hess Rise. At least two reversed-polarity intervals are identified in the early Aptian *Chiastozygus litterarius* nannoplankton zone of Hole 463. The rest of the Aptian and lower Albian sediments were found to be normally magnetized. It is impossible to construct an unambiguous reversal stratigraphy for Hole 465A, because magnetic inclinations in both the limestones and trachytes are very low. Variations in susceptibility, NRM intensity, and Curie point indicate that trachyte Units 1 and 2 are highly oxidized and have probably acquired a secondary chemical remanence. Low-titanium titanomagnetites and(or) large magnetic grains may be present in the center of Unit 3. Comparisons of paleomagnetic inclinations with current models of Pacific Plate motion produce better agreement with the Lancelot (1978) model than the Epp (1979) model. Remanence inclinations from limestones of Hole 463 are approximately 10° shallower than predicted, the difference probably being due to model errors and the effects of compaction, inclination error, the dipole offset, or off-vertical drilling.

INTRODUCTION

During DSDP Leg 62, *Glomar Challenger* occupied four sites on two major aseismic rises in the central Pacific—the Mid-Pacific Mountains and Hess Rise (Fig. 1). The major objectives of drilling were investigation of Mesozoic and Cenozoic paleoenvironments and study of the origin of the two rises.

Paleomagnetic measurements have been carried out on Aptian and Albian limestones and trachytes from Holes 463 and 465A. These studies emphasized analysis of reversal stratigraphy, estimation of site paleolatitudes, and rock magnetism of the trachytes.

METHODS

Sedimentary samples were limited to lithified and laminated intervals showing no evidence of bioturbation, drilling disturbance, or penecontemporaneous deformation. Soft and featureless oozes and chalks were avoided because they probably contain few magnetic minerals. The samples were taken from rock pieces that were too long to have rotated end for end in the core, with widths close to the diameter of the core liner, to allow for unambiguous vertical orientation. Samples were oriented by scribing an arrow on the cut surface of the core parallel to the core liner, pointing up-core. Each sample was then drilled out with a minicorer with a bit diameter of 2.54 cm, and all subsequent measurements were made relative to the orientation arrow.

All the remanence measurements were carried out either on the ship's or Southampton University's Digico spinner magnetometer. Most of the demagnetizations were undertaken at Southampton, using a Highmoor demagnetizer with a two-axis tumbler, where double demagnetizations were carried out on all samples to minimize possible acquisition of rotational remanence. A few demagnetizations were also performed on the ship's Schonstedt single-axis demagnetizer. Susceptibility measurements were made on a balanced susceptibility bridge, and Curie-point determinations were made with a horizontal-beam automatically recording Curie balance at Southampton.

Each sample was demagnetized at 50 or 100 Oersted (Oe) steps up to 400 Oe or more, but it became clear that in most limestone samples a stable component of magnetization was isolated at 150 or 200 Oe. For those samples with a less-stable response, it was also decided to use the direction after demagnetization at 150 or 200 Oe as that which best represents a stable direction. In addition, all samples were classified into four groups on the basis of their demagnetization behavior—ranging from those with magnetic directions reliable to within ±5° to those with completely unreliable directions (Table 1).

Because the core is not azimuthally oriented, inclination values alone have been used to construct a reversal stratigraphy. At low latitudes, the inclination of the geomagnetic field is close to the horizontal, and the change in inclination during a field reversal will only be a few degrees. Since the same order of magnitude of change can be brought about by secular variation (McElhinny, 1973), construction of a reversal stratigraphy in equatorial sequences is open to some doubt, except in a long core where relative declinations can also be used.

In the construction of the reversal stratigraphy presented in this paper, it was decided that a single reversed sample was not enough evidence to reliably infer that a field reversal had occurred. Consequently, all reversals shown are based on two or more samples of a given polarity.

GEOLOGIC SETTING

At Hole 463, cores were recovered from a thick section of Cretaceous limestones and chalks overlain unconformably by Cenozoic nannofossil oozes. Deposition at the site has occurred above the carbonate compensation depth throughout its history, and the site probably crossed the equator during the late Campanian or early Maastrichtian (Site 463 report, this volume). Results are presented from three lithologic units (in order of decreasing age): pelagic and clastic limestones (Unit IV), tuffaceous and carbonaceous limestones (Unit III), and cyclic multi-colored limestones (Unit II). The clastic component of Unit IV recovered near the bottom of the hole represents shallow-water stromato-

[1] *Initial Reports of the Deep Sea Drilling Project*, Volume 62.
[2] Present address: Department of Earth Sciences, Iowa State University, Ames, Iowa 50011.

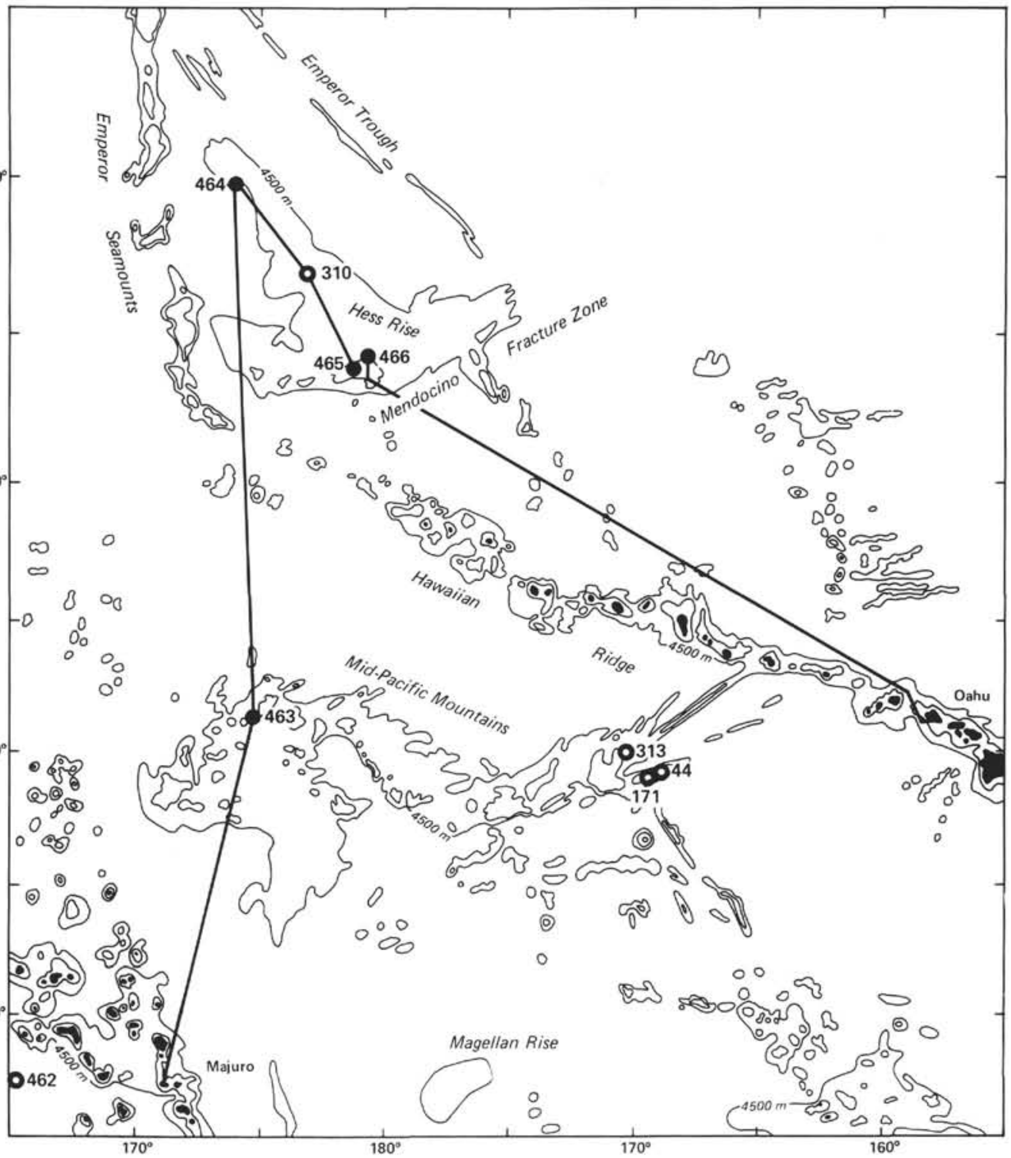

Figure 1. Location Leg 62 sites.

lite, oolite, and mollusk debris, redeposited at depths below 500 meters.

Sixty-four meters of highly oxidized trachytes and trachyte breccias were cored in Hole 465A. The sequence can be divided into five major petrologic units. From the base to the top of the sequence, they are fine-grained, amygdaloidal trachyte; coarse-grained trachyte; fine-grained, highly vesicular trachyte; medium-grained, vesicular trachyte; and brecciated trachyte (Site 465 report, this volume). The presence of large vesicles and the lack of pillow structures may indicate that the pile was extruded in a shallow subaqueous or subaerial environment. Grain-size variations allowed for the identification of some flows within each of the five units, but no continuous core was taken across an entire flow layer.

The trachytes are conformably overlain by a late Albian limestone, the lowest part of which includes reworked shallow-water debris redeposited at a depth of a few hundred meters (Site 465 report, this volume). Late in the late Albian, deposition appears to have occurred at typical continental-slope depths.

RESULTS FOR HOLE 463

Ninety-four samples from the Aptian and Albian limestones of Hole 463 were measured (Table 1). Demagnetization of Sample 463-61-1, 52–54 cm was typical of Units II and III (Fig. 2). It carries a stable component of magnetization similar in direction to the natural remanent magnetization (NRM). Sample 463-62-3, 112–114 cm (Fig. 2) differs in that the intensity of the first shore measurement (FSM, the first measurement made after returning the samples from the ship) is much higher than the NRM intensity, although it remains similar in direction. Acquisition of a secondary component of magnetization during storage and trans-

Table 1. Paleomagnetic results from limestones from Hole 463.

Sample (interval in cm)	Sub-bottom Depth (m)	NRM Intensity (10^{-6} gauss)	NRM Rel. Dec.	NRM Inc.	After Demag. Rel. Dec.	After Demag. Inc.	Reliability Category[a]	Demag. Field[b] (Oe)
463-55-1, 50–52	481.01	0.04	334.2	2.4	326.8	−19.6	1	200
56-1, 93–95	490.94	0.04	273.0	−28.6	281.3	−35.1	3	200
57-1, 27–29	499.78	0.11	136.5	−17.0	154.7	−48.3	3	200
57-1, 133–135	500.84	0.21	241.0	−10.4	234.1	−30.2	1	200
57-2, 26–28	501.27	0.98	30.9	−22.0	37.8	−30.9	1	200
57-2, 66–68	501.67	0.24	346.2	−20.1	348.0	−29.6	1	200
58-1, 5–7	509.06	5.62	109.4	−21.2	107.4	−21.9	1	200
58-2, 83–85	511.34	10.72	308.6	−21.5	307.9	−20.7	1	200
58-3, 5–7	512.06	2.88	251.6	−36.1	245.4	−24.8	1	200
59-2, 100–102	521.01	6.40	226.0	−32.5	222.2	−31.2	1	200
59-3, 147–149	522.98	5.54	67.1	−36.4	72.2	−42.5	1	200
59-4, 15–17	523.16	4.27	136.1	−31.0	142.8	−22.9	2	200
59,CC, 4–6	523.35	4.96	107.0	−24.5	105.9	−34.5	1	200
60-1, 9–11	528.10	11.45	320.7	−24.2	—	—	—	—
60-2, 27–29	529.78	11.99	242.7	−38.0	242.9	−40.2	1	200
60-4, 45–47	532.96	22.75	21.7	−38.8	22.0	−24.4	1	200*
60-4, 89–91	533.40	8.38	77.2	−39.8	78.9	−28.4	1	200
61-1, 52–54	536.03	4.07	26.2	−32.6	30.5	−29.2	1	200
61-1, 76–78	536.27	3.16	139.5	−32.5	139.1	−39.0	1	200
62-1, 5–7	537.56	2.93	114.9	−54.0	124.2	−46.0	1	200
62-1, 125–127	538.76	0.65	344.3	−24.5	337.9	−32.7	1	200
62-2, 82–84	539.83	1.02	48.7	−43.4	50.0	−31.9	1	200
62-3, 7–9	540.58	0.54	190.5	−30.2	201.7	−39.4	1	200
62-3, 112–114	541.63	1.16	347.3	−31.4	352.1	−26.6	1	200
63-1, 81–83	547.82	0.75	136.6	−17.4	136.2	−25.2	1	200
63-3, 12–14	550.13	0.46	74.0	−15.5	76.5	−34.0	1	200
63,CC, 23–25	550.74	4.20	348.7	−10.8	355.1	−28.5	1	200
64-1, 2–4	556.53	3.29	77.0	−25.7	74.0	−36.8	1	150*
64-1, 5–7	556.56	0.73	72.6	−26.8	66.0	−30.7	1	200
64-1, 9–11	556.60	0.40	76.4	−16.1	58.6	−31.0	2	200
64-1, 15–17	556.66	0.44	137.7	−18.5	150.6	−33.6	1	200
64-1, 21–23	556.72	0.47	139.1	−16.0	142.3	−31.7	2	200
64-2, 15–17	558.16	4.29	302.6	−13.2	305.1	−34.1	1	200
64-2, 114–116	559.15	3.48	63.0	−27.8	69.5	−43.4	2	200
64-3, 67–69	560.18	1.63	259.3	−9.4	260.2	−27.6	1	200
65-1, 64–66	566.65	1.51	341.8	−10.0	348.8	−28.7	1	200
65-2, 21–23	567.72	3.30	35.8	−15.1	37.2	−14.1	1	200*
65,CC, 18–20	569.59	2.19	207.4	−17.4	—	—	—	—
66-1, 17–19	575.68	0.88	187.8	−28.1	192.5	−13.7	2	700
66-2, 21–23	577.22	1.82	176.8	−10.0	184.4	−26.7	1	200
66-3, 35–37	578.86	0.34	312.6	−4.6	328.9	−43.6	2	200
67-1, 68–70	585.69	0.15	39.0	−7.0	40.4	−30.5	3	200
67-1, 78–80	585.79	0.15	130.7	−24.1	98.8	−28.9	2	200
67-1, 105–107	586.06	0.33	75.8	−9.0	97.4	5.7	2	200
67-1, 121–123	586.22	0.16	228.0	5.2	221.7	5.8	2	100
67-1, 128–130	586.29	0.15	311.1	11.0	329.1	11.9	2	100*
67-1, 136–138	586.37	0.06	318.4	7.8	318.0	−34.3	2	150
67-2, 9–11	586.60	0.39	292.1	−8.6	290.0	−25.7	1	200
67-2, 29–31	586.80	0.37	189.5	−1.3	184.1	−30.5	1	200
67-2, 83–85	587.34	0.15	21.0	−26.5	26.4	−29.2	1	200
67-2, 120–122	587.71	0.17	273.0	−6.3	280.6	−16.0	1	150
68-1, 15–17	594.66	0.18	225.1	−18.6	221.2	−32.5	1	200
69-1, 88–90	604.89	0.40	295.6	−9.5	282.6	−21.8	2	200
69-1, 141–143	605.42	0.13	111.0	−1.9	121.4	−22.2	1	200
69-2, 134–136	606.85	1.29	66.2	−28.2	67.3	−26.0	1	200
69-2, 141–143	606.92	0.10	53.2	−18.4	58.8	−15.7	1	200
69-3, 12–14	607.13	1.29	271.5	−29.4	258.6	−7.7	1	200
70-1, 9–11	613.60	0.13	38.7	−26.5	69.5	−29.5	1	200
70-1, 125–127	614.76	0.12	280.8	−0.3	278.6	−10.4	1	200
70-2, 48–50	615.49	0.04	6.5	−16.2	334.2	−32.2	2	200
70-3, 39–41	616.90	0.01	200.4	−24.5	132.0	−17.2	2	150
70-4, 30–32	618.31	0.98	18.1	−12.9	12.2	−8.0	1	200
70-5, 14–16	619.65	0.04	293.6	−21.0	—	—	—	—
70-5, 130–132	620.81	0.08	310.4	−24.1	—	—	—	—
70-6, 50–52	621.51	0.06	50.3	−54.1	—	—	—	—
70,CC, 18–20	622.99	1.57	185.4	−23.9	191.5	−33.5	2	200
71-1, 36–38	623.37	0.11	98.6	−25.9	111.2	−29.0	2	200
71-1, 74–76	623.75	0.10	180.6	−19.7	185.2	−25.6	1	200
71-2, 77–79	625.28	0.37	27.9	−13.9	10.7	−6.1	1	200
71-2, 118–120	625.69	0.07	59.0	−33.1	66.9	−20.6	1	200
71-3, 79–81	626.80	0.18	164.5	−13.9	162.5	−24.0	1	200
71-4, 95–97	628.46	0.11	42.8	−28.9	55.5	−19.1	1	200
71-1, 106–108	633.57	0.36	309.3	−76.9	61.5	−28.2	3	200
72-2, 43–45	634.44	0.13	5.5	−37.2	—	—	—	—
72-2, 120–122	635.21	0.10	41.0	−61.5	—	—	—	—
72-3, 56–58	636.07	0.18	341.1	−46.9	—	—	—	—
72-3, 80–82	636.31	0.23	46.1	−18.2	58.0	19.4	1	200
72-3, 136–138	636.87	0.10	135.4	29.6	—	—	—	—
72-4, 33–35	637.34	0.30	35.0	−38.5	—	—	—	—
72-4, 77–79	637.78	0.06	323.0	−12.9	310.1	9.0	3	150
72-5, 10–12	638.61	0.05	292.4	31.8	171.5	48.3	3	200
72-5, 28–30	638.79	0.12	295.9	−48.7	277.0	−36.0	2	200
73-1, 97–99	642.98	0.24	249.5	−4.8	231.5	−7.7	2	200
73-2, 91–93	644.42	0.48	244.2	−17.9	197.5	−17.8	2	200
74-2, 4–6	653.05	0.02	350.0	−1.3	168.9	−9.2	2	50
75-1, 8–10	661.09	0.04	65.2	15.2	—	—	—	—
75-1, 35–37	661.36	0.12	325.5	−17.0	2.6	−6.1	2	200
76-1, 19–21	670.70	0.06	325.8	−23.1	319.0	−38.1	1	200
76-1, 63–65	671.14	0.18	204.8	−22.7	215.0	−34.7	1	200
77-1, 37–39	680.38	0.18	42.5	18.5	85.6	22.2	3	150*
77-1, 66–68	680.67	0.12	66.7	−56.0	—	—	—	—
77-1, 87–89	680.88	0.16	31.2	27.2	—	—	—	—
78-1, 24–26	689.75	0.16	14.4	39.7	—	—	—	—
78-1, 94–96	690.45	0.04	352.5	−15.8	—	—	—	—
78-1, 43–45	691.44	471.50	322.4	27.3	—	—	—	—

[a] Reliability cateogories are (1) ±5°, (2) ±15°, (3) generally unreliable (intensity close to instrument noise level), but with some indication of a stable endpoint, (4) unreliable.
[b] Asterisk indicates demagnetization performed aboard ship; others were performed on shore.

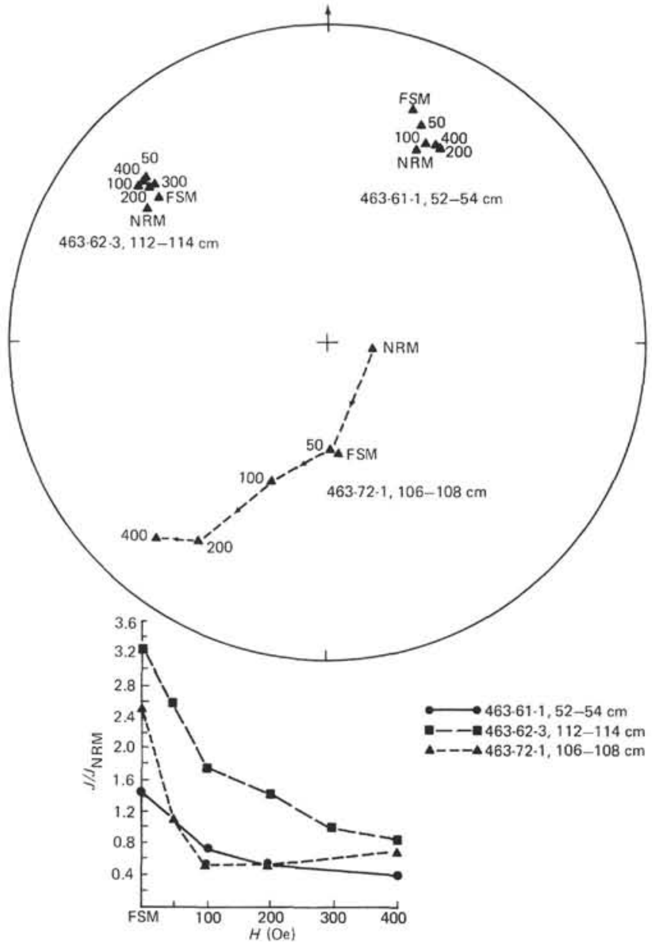

Figure 2. Representative demagnetizations of samples from Hole 463, plotted on an equal-area stereographic projection. FSM indicates the direction of the first shore measurement. Field strengths in Oe. Triangles—upper hemisphere.

portation is a possible cause, but it would also probably be different in direction from the NRM. It seems more likely that the calibration of the shipboard and shore-based magnetometers may have differed. It is thought that the shore-based intensity results are more reliable, because the shipboard magnetometer had high and variable noise levels.

Many of the samples of the pelagic and clastic limestones (Unit IV) had very low NRM intensities below the noise level of the shipboard magnetometer and close to that of the shore laboratory magnetometer. A few samples did carry a remanence strong enough to be demagnetized. The NRM direction of Sample 463-72-1, 106–108 cm (Fig. 2) is steeply inclined, but demagnetization reveals a more stable component at lower inclinations, similar to those of samples from the overlying units. This sample had acquired a strong secondary remanence that was successfully removed by demagnetization.

The Barremian section at Hole 463 has been sampled, but was very weakly magnetized. These samples await measurement on more-sensitive equipment.

Looking at the results in general, inclination values from Hole 463 were steepened by about 10° after demagnetization (Fig. 3), probably indicating removal of a secondary component with positive inclination, perhaps paralleling the present-day field. The dominance of negative inclinations reflects the fact that the Aptian and Albian are made up of long intervals of normal polarity.

RESULTS FOR HOLE 465A

Twenty-six samples of late Albian limestone and twenty-five of trachyte from Hole 465A were measured (Table 2). Most of the limestones carry a stable direction of magnetization with low inclination, shallower than the NRM direction. Sample 465A-33-1, 25–27 cm has a stable direction with negative inclination which is revealed only after demagnetization to 150 Oe (Fig. 4). Sample 465A-38-2, 95–97 cm also has a low inclination, but it is positive instead of negative. Several samples have higher inclinations than these, but most fall in reliability category 3 (Table 1), indicating that a secondary component may not have been removed completely during demagnetization. Looking at the results of demagnetization as a whole (Fig. 5), a slight decrease in positive inclination after demagnetization probably represents the removal of a secondary component paralleling the present geomagnetic field.

All the trachyte samples carry a stable component of magnetization close to the NRM direction, but with very low inclinations of variable sign (Fig. 6). Two results merit further attention. First, inclination values in Unit 1 and most of Unit 2 are greater than those in other units (Fig. 7), and correlate with extremely low values of susceptibility and NRM intensity (Fig. 8; Table 3). Second, susceptibility and NRM intensity show a marked peak at the center of Unit 3.

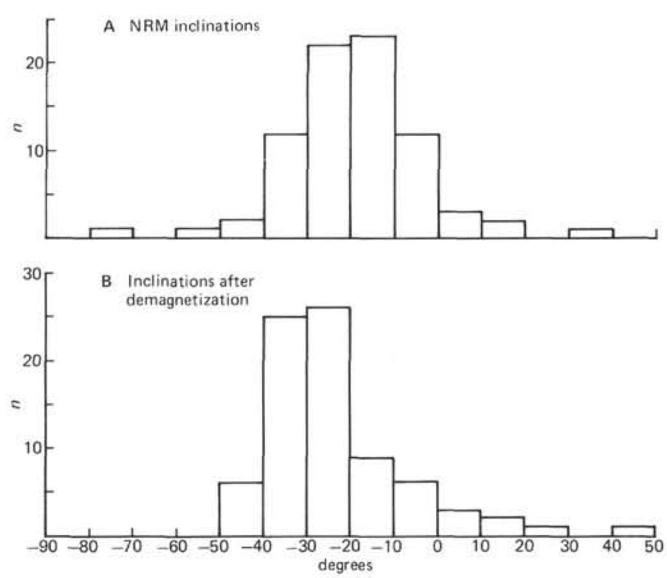

Figure 3. Histograms of inclination data from Cores 55 through 78, Hole 463. A. NRM. B. After partial demagnetization at 150 or 200 Oe. (See Table 1 for field strengths.)

Table 2. Paleomagnetic results from limestones and trachytes from Hole 465A.

Sample (interval in cm)	Sub-bottom Depth (m)	NRM Intensity (10^{-6} gauss)	NRM Rel. Dec.	NRM Inc.	After Demag. Rel. Dec.	After Demag. Inc.	Reliablity Category[a]	Demag. Field[a] (Oe)
465A-26-1, 52–54	277.03	1.10	64.2	5.5	62.9	9.4	1	200*
26-1, 106–108	277.57	0.11	323.9	63.2	—	—	—	—
27-1, 71–73	286.72	0.42	203.3	17.2	224.9	20.6	3	100*
27-2, 100–102	288.51	0.49	48.1	18.5	50.2	35.7	2	200*
28-1, 112–114	296.63	0.54	245.5	−28.4	250.4	15.6	2	400
28-2, 15–17	297.16	0.12	57.3	2.2	47.7	11.2	2	200
29-1, 88–90	305.89	0.03	205.7	18.4	219.6	−3.3	2	600
29-1, 144–146	306.45	0.09	315.7	38.5	—	—	—	—
30-1, 76–78	315.27	0.07	65.6	20.5	59.0	15.9	2	150
31-1, 32–34	324.33	1.46	215.5	−6.1	229.4	3.1	1	200
32-1, 108–110	334.59	0.17	301.9	21.9	320.4	3.2	1	200
33-1, 25–27	343.26	0.16	4.1	17.2	5.6	−0.6	1	200
33-2, 52–54	345.03	0.04	236.7	8.5	247.0	3.3	1	200
34-1, 47–49	352.98	0.10	187.5	−17.7	179.4	−2.3	1	200
34-2, 35–37	354.36	0.01	83.7	12.2	50.3	42.7	3	50*
35-1, 30–32	362.31	0.06	26.1	1.3	54.7	−1.4	1	200
36-1, 78–80	372.29	0.01	26.1	−7.0	—	—	—	—
36-2, 78–80	373.79	0.03	2.5	65.6	25.5	40.8	3	50*
37-1, 71–73	381.72	0.11	248.3	4.5	252.5	4.8	2	200
37-2, 20–22	382.71	0.10	254.9	58.5	354.9	7.3	3	50*
38-1, 46–48	390.97	0.09	81.7	47.0	72.3	69.0	3	50*
38-2, 95–97	392.96	0.33	184.5	13.7	184.5	8.0	2	150
39-1, 55–57	400.56	0.03	279.6	5.4	265.0	16.0	3	50
39-2, 85–87	402.36	0.24	79.9	7.1	77.0	−1.6	1	200
40-1, 95–97	410.46	0.01	353.0	−35.8	318.2	18.5	2	100
40-2, 59–61	411.60	0.57	349.9	14.5	348.5	1.4	2	200*
40-2, 107–109	412.08	0.02	85.3	−18.0	—	—	—	—
40-3, 32–34	412.83	0.11	313.7	−1.2	—	—	—	—
41-1, 132–134	420.33	1.96	76.9	22.7	69.4	33.7	2	200
41-2, 82–84	421.33	14.38	213.5	29.0	211.6	26.2	2	200*
41-3, 31–33	422.32	8.89	336.4	26.2	319.2	25.1	2	350*
42-1, 126–128	429.77	9.63	187.1	13.2	182.7	12.6	2	300*
42-2, 83–85	430.84	19.34	69.9	31.2	51.8	22.5	2	200
42-3, 95–97	432.46	104.40	31.4	30.9	28.6	35.6	2	200*
43-1, 124–126	439.25	30.17	2.9	−0.3	1.5	−1.5	1	200*
43-2, 131–133	440.82	283.20	295.8	−1.0	287.3	−4.5	1	500
44-1, 108–110	448.59	205.10	16.6	5.2	16.8	13.9	2	300*
44-2, 78–80	449.79	508.70	25.9	−10.1	22.3	−1.2	2	200*
44-3, 91–93	451.42	730.4	233.0	−12.0	229.6	−5.5	1	300*
44-3, 124–126	451.75	598.9	194.4	−11.0	195.7	−6.2	2	200*
45-1, 2–4	457.03	701.6	139.7	−8.0	140.4	−6.6	1	300*
45-1, 59–61	457.60	970.7	98.7	−11.4	99.5	−9.6	2	200*
45-2, 19–21	458.70	464.4	75.1	−12.7	80.7	−5.3	1	300*
45-2, 129–131	459.80	691.0	235.1	−4.6	234.0	−8.9	1	200*
45-3, 112–114	461.13	325.1	64.7	−2.8	63.7	−0.8	1	300*
45-4, 49–51	462.00	110.8	254.4	−3.1	253.1	−7.5	1	400*
45-4, 111–113	462.62	371.9	66.2	9.4	86.0	4.6	2	200*
46-1, 51–53	467.02	236.1	343.3	8.4	338.4	17.8	1	300*
46-2, 26–28	468.27	374.1	90.6	−5.6	85.2	−12.4	1	400*
46-2, 116–118	469.17	359.3	147.4	−3.8	150.9	2.5	1	300*
46-3, 31–33	469.82	409.8	16.4	6.5	12.9	9.8	1	200*

[a] See notes for Table 1.

The higher inclination values might suggest that Units 1 and 2 were formed at higher latitudes than Units 3, 4, and 5. This could be explained by a hiatus in eruption lasting several million years, while the Pacific plate moved northward by approximately 10°, or by a precipitous increase in the rate of spreading. Both of these explanations seem unlikely. Alternatively, the apparent change in inclination could be caused by inadequate averaging of secular variation, or by relative tilting of the different units. However, it seems most likely that the acquisition of a strong chemical remanent magnetization (CRM) during oxidation has played an important role in altering the direction of remanence in Units 1 and 2.

The effects of submarine oxidation on the titanomagnetite series are well documented. Shrinkage and cracking reduce the effective magnetic-grain size, although the visible grain size may remain constant (Ade-Hall et al., 1975a). Magnetic susceptibility would probably decrease as a result; although susceptibility may be controlled by a number of factors, such as magnetic mineral content and concentration and crystal-lattice imperfections, variations in grain size often mask their effects (Marshall, 1978). Titanomagnetite is oxidized to titanomaghemite as Fe^{+2} ions leave the octahedral sites of the crystal lattice. The consequent vacancies reduce the cell size and increase the concentration of the strongly interactive Fe^{+3} ions (Marshall, 1978). This can result in a decrease in magnetic intensity due to the loss of iron, and an increase in the Curie point. In addition, it has been shown experimentally (Johnson and Merril, 1973) that in a natural titanomagnetite low-temperature oxidation can produce a chemical remanence more stable than the original natural remanence.

The Curie point of a rock sample is a sensitive indicator of oxidation (Readman and O'Reilly, 1972). However, it also varies with mineral composition, decreasing with increasing titanium content in the original titanomagnetite (e.g., McElhinny, 1973), which in turn can depend on the crystallization temperature of the parent magma, and also on subsequent high-temperature oxidation (Larson et al., 1969). Only with a knowledge of the crystal-lattice dimensions can the amount of oxidation be accurately calculated. However, by studying the changes in saturation magnetization by heating a sample to its Curie point much can still be learned.

Oxidized submarine lavas have a characteristic heating and cooling curve (Ozima and Ozima, 1971; Sakamoto et al., 1968). Usually these rocks consist of nonstoichiometric titanomaghemite with a Curie point be-

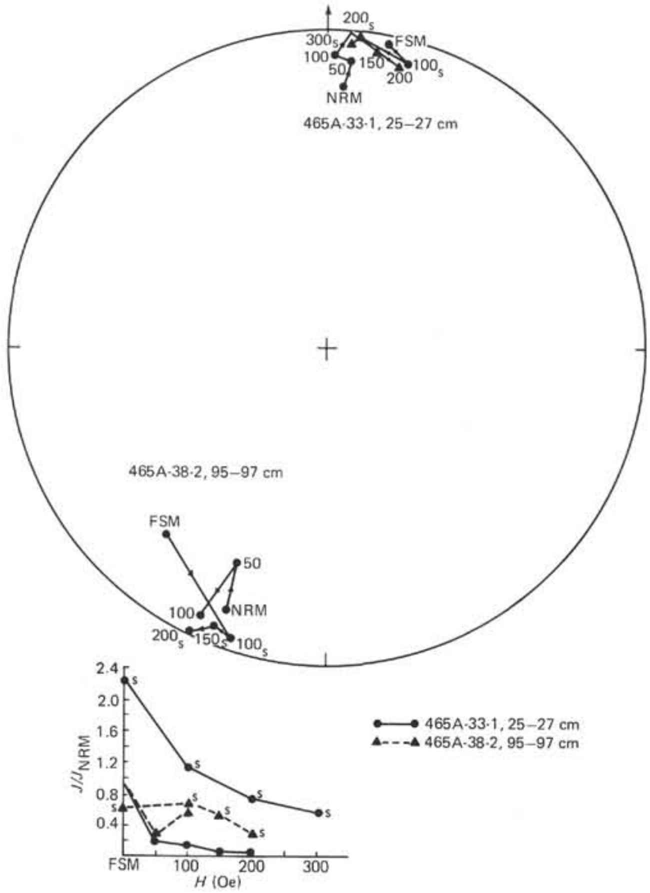

Figure 4. Representative demagnetizations of limestone from Hole 465A plotted on an equal-area stereographic projection. Labels as in Figure 1. Subscript "s" denotes shore-based demagnetization results. Triangles—upper hemisphere. Points—lower hemisphere.

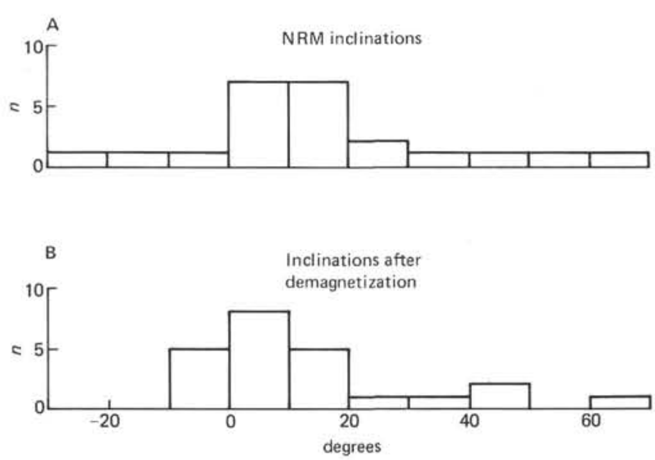

Figure 5. Histograms of inclinations of limestones from Cores 26 to 40, Hole 465A. A. NRM. B. After partial demagnetization at 150 or 200 Oe. (See Table 2.)

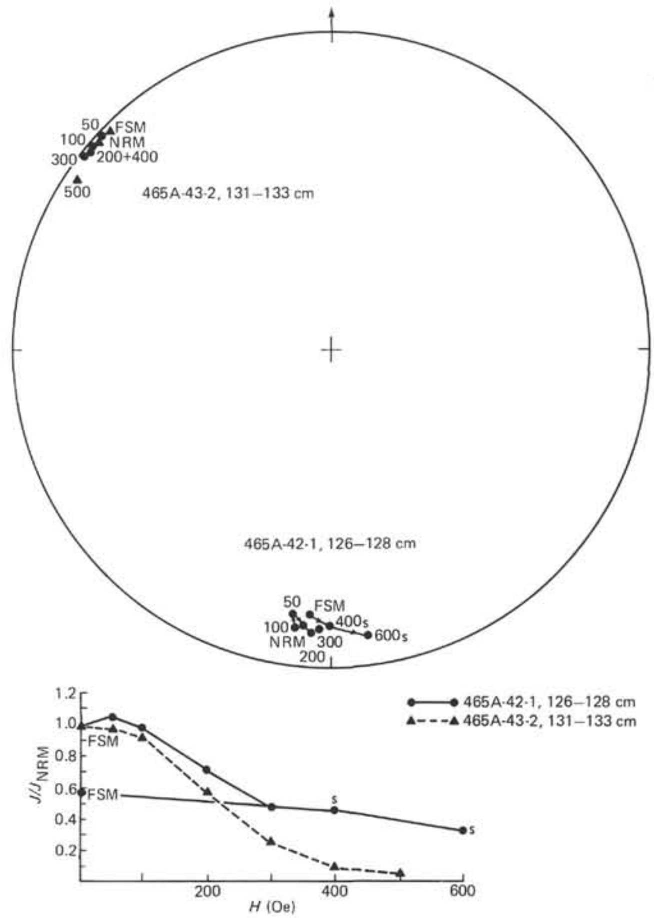

Figure 6. Representative demagnetization of trachyte samples from Hole 465A plotted on an equal-area stereographic projection. Labels as in Figures 1 and 4.

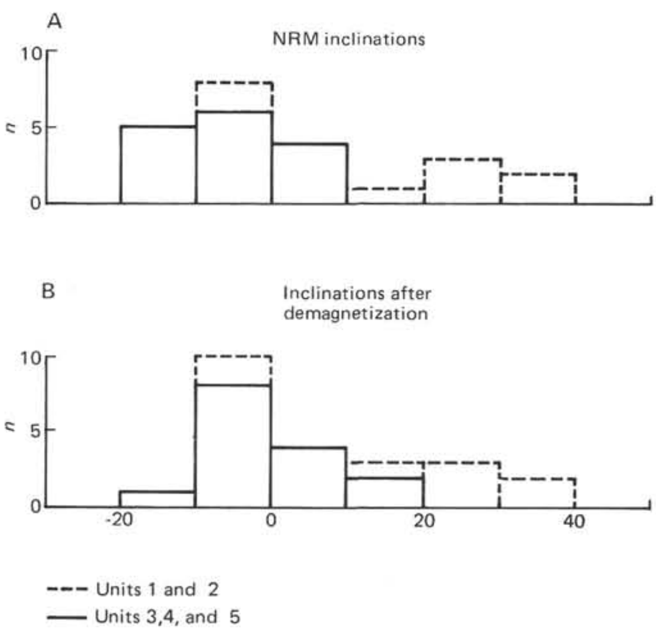

Figure 7. Histograms of inclinations of trachytes from Hole 465A. A. NRM. B. After partial demagnetization. (See Table 2.)

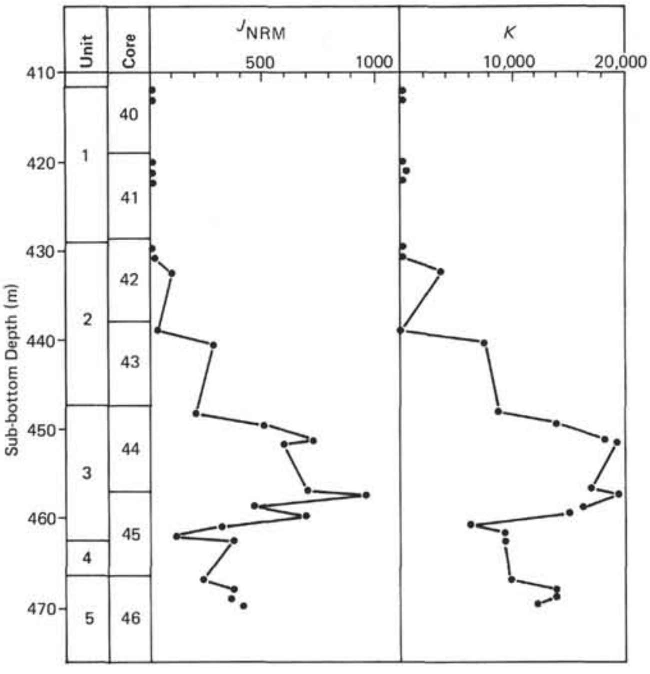

Figure 8. Down-hole variation of NRM intensity and susceptibility for trachytes from Hole 465A.

Table 3. NRM intensities, susceptibilities, and median destructive fields for trachytes from Hole 465A.

Sample (interval in cm)	Sub-bottom Depth (m)	NRM Intensity (10^{-6} emu)	Susceptibility[a] (10^{-6} emu/Oe)	Median Destructive Field (Oe)
456A-40-2, 107–109	412.08	0.02	118.5	—
40-3, 32–34	412.83	0.11	101.1	—
41-1, 132–134	420.33	1.96	132.5	75
41-2, 82–84	421.33	14.38	432.2	275
41-3, 31–33	422.32	8.89	174.3	325
42-1, 126–128	429.77	9.63	90.6	300
42-2, 83–85	430.84	19.34	219.6	250
42-3, 95–97	432.46	104.40	3710.0	250
43-1, 124–126	439.25	30.17	355.5	300
43-2, 131–133	440.82	283.20	7574.2	225
44-1, 108–110	448.59	205.10	8836.2	225
44-2, 78–80	449.79	508.70	13886.0	150
44-3, 91–93	451.42	730.40	18304.3	175
44-3, 124–126	451.75	598.90	19566.7	125
45-1, 2–4	457.03	701.60	17041.9	175
45-1, 59–61	457.60	970.70	19566.7	150
45-2, 19–21	458.70	464.40	16410.8	175
45-2, 129–131	459.80	691.00	15148.4	175
45-3, 112–114	461.13	325.10	6311.8	200
45-4, 49–51	462.00	110.8	9467.7	225
45-4, 111–113	462.62	371.9	9563.5	175
46-1, 51–53	467.02	236.1	10098.9	225
46-2, 26–28	468.27	374.1	13886.0	175
46-2, 116–118	469.17	359.3	13886.0	200
46-3, 31–33	469.82	409.8	12623.7	175

[a] Not corrected for sample volume.

tween 100 and 400°C (Fig. 9A). As the sample is heated in a vacuum, a hump in saturation magnetization occurs above this temperature as the titanomaghemite unmixes to form two phases, a titanium-poor, nearly pure magnetite, and a titanium-rich hemo-ilmenite or pseudobrookite. A second Curie point at 570°C represents the newly formed magnetite, whose magnetic properties dominate the titanium-rich phase. On cooling, an upshift in the curve reflects the greater saturation magnetization of the magnetite compared to the original titanomaghemite.

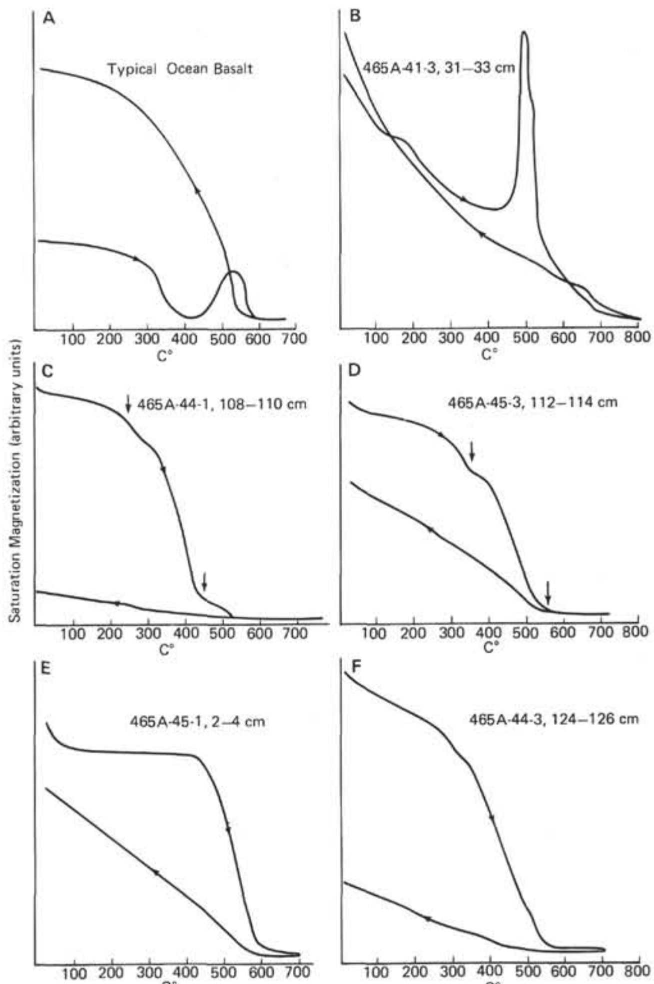

Figure 9. Thermomagnetic curves of (A) typical ocean basalt in a vacuum (Marshall, 1978), and (B–F) selected trachyte samples from Hole 465A. Vertical arrows indicate inferred Curie points. Maximum uncertainty in temperature scale (due to relative position of sample and thermocouple) is 25°C.

All the thermomagnetic measurements described below were made in air, which means that a hump in the heating curve and upshift of the cooling curve can also be due to the oxidation of a titanomagnetite to titanomaghemite during the initial part of the heating cycle and does not necessarily indicate that the sample was naturally oxidized. Figure 9B shows the results of heating and cooling of Sample 465A-41-3, 31–33 cm from Unit 1. This sample shows some, but not all the characteristics of titanomaghemite, discussed above. It displays an initial low Curie point at about 125°C and striking peak in saturation magnetization at 500°C, indicating production of magnetite with a second, higher Curie point between 550 and 600°C. However, the downshift in the cooling curve is apparent, possibly due to a number of processes, such as partial reduction during cooling (Marshall, 1978), or an order–disorder phenomenon (Grommé et al., 1969; Larson et al., 1969). Because the sample was heated to over 700°C, it is also possible that the magnetite itself was oxidized to hematite, causing a reduction in saturation magnetization.

Although this result is not conclusive in indicating the existence of a naturally oxidized titanomaghemite, when considered with the extremely low susceptibility and NRM intensity values, it seems likely that Units 1 and 2 are more-oxidized than the rest of the sequence, and that they may have been remagnetized. The lower two samples of Unit 2 have inclinations similar to those of samples from Unit 3, and somewhat higher susceptibilities and intensities than the rest of Unit 2. Thus, the depth of penetration of this inferred intense oxidation is tentatively placed at the top of Core 43. Increased fracturing associated with the upper part of the sequence probably provided avenues for oxidizing sea water.

The other striking result from the trachyte sequence is the large peak in intensity and susceptibility at the center of Unit 3 (Fig. 8, Table 3). Again, intense low-temperature oxidation at the upper and lower margins of Unit 3 could effectively reduce intensities and susceptibilities. Alternatively, Unit 3 may be a single cooling unit, and high susceptibilities could reflect large grain sizes (as the center cooled more slowly than the edges). A third model can also be considered, in which the variation in magnetic properties could be brought about by differing amounts of titanium in the titanomagnetites at different levels in the unit. If this were the case, low-titanium, nearly pure magnetite would be expected in the center, and titanomagnetites with higher concentrations of titanium would occur at the margins (Nagata, 1961). Results of thermomagnetic analyses (Fig. 9) allow for an assessment of these different models.

Two samples taken from the upper and lower margins of Unit 3 show a similar thermomagnetic response (Figs. 9C and 9D). Each displays two Curie points at 250 to 350°C and 450 to 550°C, indicated by the vertical arrows near the curves. Saturation magnetization decreases upon cooling, and there is no evidence of magnetite formation. The two Curie temperatures reflect the presence of two magnetic phases: the lower point probably reflects an unoxidized, high-Ti titanomagnetite, and the other either an oxidation product of the first or a fresh, low-Ti titanomagnetite.

Two samples from the center of Unit 3 (Figs. 9E and F) are similar to each other and different from those from the margin, in that they have a single dominant Curie point near 570°C, probably indicative of fresh, very low-Ti titanomagnetite. The very high values of susceptibility and NRM intensity for these samples confirm that the material is probably unoxidized. The downshift in the cooling curve may be caused by the factors already discussed.

Curie points suggest a variation in Ti content through Unit 3, which could results from changes in the crystallization temperature of the parent magma, or high-temperature oxidation (Larson et al., 1969). If low-temperature oxidation has occurred, it was probably less intense than in Units 1 and 2, because there is no associated change in inclination. However, it is difficult to envision how oxidizing sea water could gain access to the base of the unit without affecting its center. Grain-size variation cannot be ruled out, as previously mentioned, and if it is responsible for the observed magnetic properties, Unit 3 may indeed represent, magnetically, a single cooling unit.

REVERSAL STRATIGRAPHY

The entire Aptian and lower Albian sequences at Hole 463 have been sampled (Table 1, Fig. 10), and the section was found to have dominantly negative inclinations, indicative of normal polarity because the site was in the southern hemisphere. At least two reversed intervals were detected, both in the *Chiastozygus litterarius* Zone of the early Aptian (Cores 67 and 72). The upper interval is defined by three demagnetized samples, and the other by three demagnetized samples and one undemagnetized. A third reversely magnetized interval may occur in Cores 77 and 78, but it is defined by only one demagnetized and three undemagnetized samples. The undemagnetized samples have very weak intensities and are being reserved for future measurements on more sensitive equipment.

Stable inclinations are low and variable in sign at Hole 465A (Fig. 11). This site was probably close to the

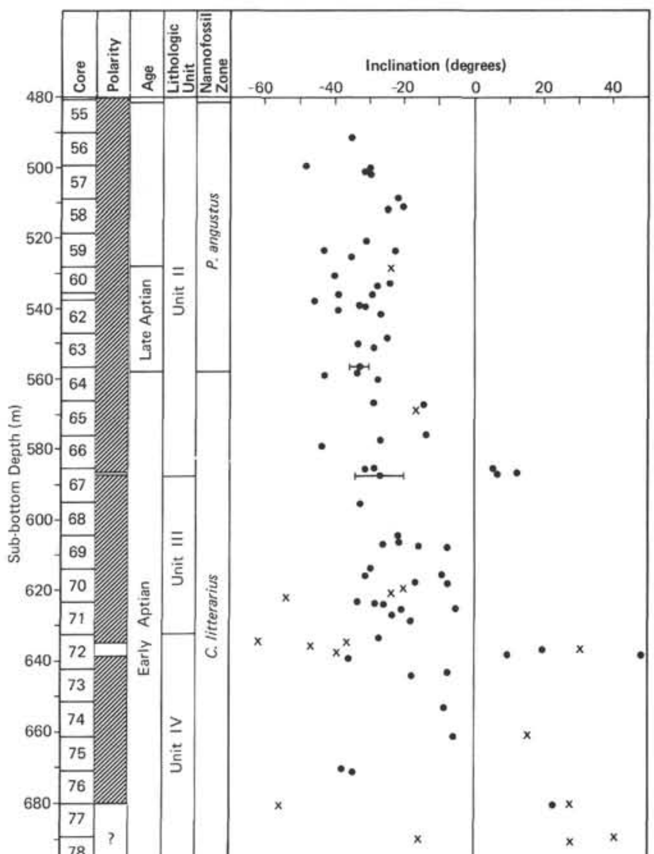

Figure 10. Down-hole variation of inclination and inferred polarity intervals for limestone from Hole 463. Shaded intervals represent normal polarities. Crosses represent NRM inclinations; points represent inclinations after partial demagnetization. Error bars represent standard deviation of a mean inclination of five closely spaced samples.

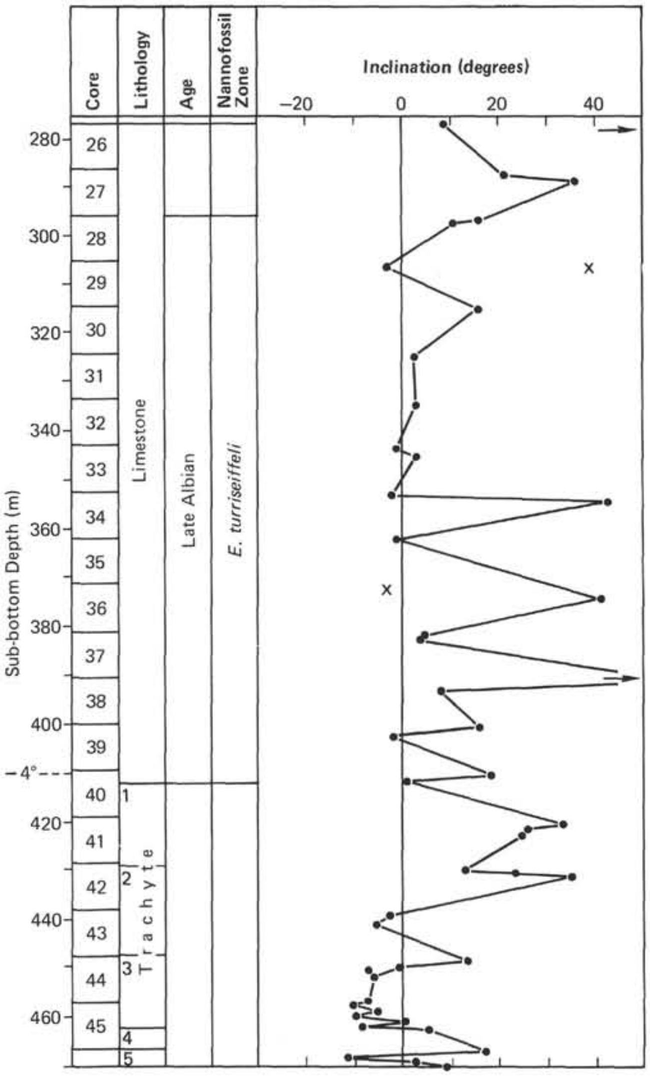

Figure 11. Down-hole variation of inclination for limestone and trachytes from Hole 465A. The hole is 4° off vertical at Core 40. Crosses represent NRM inclinations; points represent inclinations after partial demagnetization.

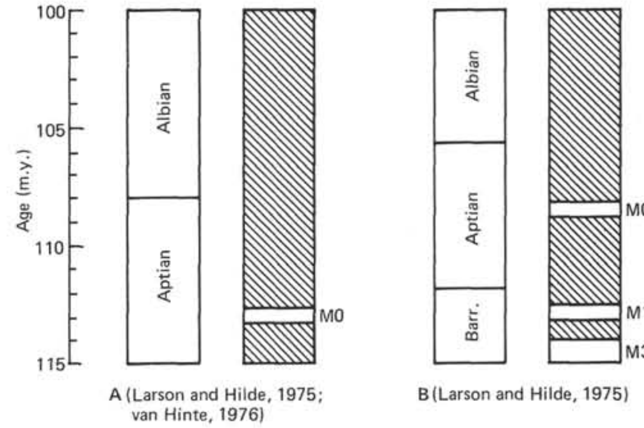

Figure 12. Marine magnetic-anomaly time scales for the Aptian and Albian. Shaded intervals represent normal polarity. A. Larson and Hilde (1975), calibrated according to van Hinte (1976). B. Larson and Hilde (1975), calibrated according to Geological Society of London (1964).

Equator during the late Albian (see next section), and, as discussed earlier, this makes it difficult to construct a reversal stratigraphy. Sediment samples have predominantly positive inclinations, and trachytes (Units III to V) have mostly negative inclinations.

Larson and Hilde (1975) have constructed a Mesozoic reversal time scale based on the "M" marine magnetic-anomaly sequence of the Hawaiian lineations in the north Pacific (Fig. 12B). This sequence was tied to the time scale of the Geological Society of London (1964) by age determinations on the normal intervals between Anomalies M7 and M8, and Anomalies M24 and M25, determined from drilling at DSDP Holes 166 and 105, respectively; the scheme assumes that the lineations were formed during a period of constant spreading at a rate of 3.29 cm/yr. The Larson and Hilde (1975) time scale gives marine magnetic anomaly M0 a middle Aptian date. Using a more recent numerical time scale (van Hinte, 1976) the sequence of M reversals analyzed by Larson and Hilde (1975) can be recalibrated, with a change in the assumed constant spreading rate to 4.15 cm/yr (Fig. 12A). This would place M0 in the early Aptian.

Reversal time scales based on constant spreading rates can be regarded only as first approximations to the real reversal stratigraphy. The original reversal time scale for the Cenozoic (Heirtzler et al., 1968) was also based on an assumption of a constant spreading rate in the South Atlantic, but later studies have shown that at least two changes in spreading rate have occurred (e.g., Hailwood et al., 1979). In addition, other studies do not agree with these proposed ages for anomaly M0. It has been dated as late Aptian (van Hinte, 1976), and, in a paleomagnetic study of pelagic carbonates in the Umbrian Alps in northern Italy, Lowrie et al (1979) correlated it with a reversed interval near the Aptian/Barremian boundary.

Thick sequences of Aptian and Albian sediments were cored in DSDP Holes 398, 400A, and 402A, on the western continental margin of Europe, and a paleomagnetic study showed no evidence of a reversed interval in the Aptian or near the Aptian/Albian boundary which could correlate with M0 (Hailwood et al., 1980). It is possible that its absence is due to a combination of coring gaps and sedimentary hiatuses and, by default, it was assigned a late Aptian age. Short-period reversals in the upper Albian at Holes 400A and 402A correlate well with the Site 263 mixed-polarity zone (Green and Brecher, 1974; Jarrard, 1974).

In sharp contrast to Hailwood et al. (1980), Keating and Helsley (1978a) have tentatively identified at least eight reversed intervals in Aptian and Albian sediments from the Atlantic continental margins of Africa and the United States, drilled on DSDP Legs 40, 41, 43, and 44. As they point out, some of their conclusions are based on NRM data alone, and many of their reversals are poorly dated. However, at least four reversals based on demagnetized results have been well dated. In the Aptian, reversely magnetized samples were found in the calcareous nannofossil *Chiastozygus litterarius* Zone of the early Aptian at Hole 361 (Keating and Helsley, 1978b), and in the late Aptian at Hole 369 (Keating and Helsley, 1978c). Lowrie et al. (1979) also report a late Aptian event. In the Albian, Keating and Helsley (1978b) show a reversal at the very top of the *Parhabdolithus angustus* Zone of the early Albian at Hole 361, and in the lower part of the *Eiffellithus turriseiffeli* Zone of the upper Albian. Although the Keating and Helsley (1978b) early Aptian reversal may correlate with M0, the rest do not appear to have been recorded in the ocean crust, perhaps indicating that each was relatively short-lived (Keating and Helsley, 1979).

One or more of the early Aptian reversals of Hole 463 probably correlates with anomaly M0 and the Hole 361 reversal. The lack of reversals in the upper Aptian and lower Albian is in agreement with the results from Holes 398, 400A, and 402A, but non-recovery has left some unsampled gaps.

The predominance of negative inclinations in the trachytes and positive inclinations in the sediments from Hole 465A may be evidence that they were formed during different polarity intervals, or different parts of the secular variation cycle. In addition, the change in inclination could be a result of the northerly motion of the Pacific Plate during the formation of the trachytes and the sediments.

PALEOLATITUDE ESTIMATES

The equation

$$\tan I = 2 \tan \lambda$$

relates the inclination of the geomagnetic field, I, to latitude, λ, assuming that the field is axial and geocentric. By replacing I with the inclination of remanence from a particular rock unit, it is possible to estimate the latitude at which the magnetization was acquired. It is clear that this method is only a first approximation, because it has been shown that the long-term geomagnetic field may not be geocentric (Wilson, 1970; Cox, 1975; Hailwood, 1977).

In addition, a number of other effects can impart an error in the acquisition of inclinations in sedimentary and igneous rocks. For example, an inclination error in coarse-grained sediments has been known for some time (e.g., King, 1955; Griffiths et al., 1960) although it is less common in finer-grained pelagic sediments, where post-depositional rotation is thought to re-align the magnetic grains (Løvlie, 1974, 1976). Also, compaction after dewatering can make inclination values too shallow (Keen, 1963). Differences between remanent inclination and the present geomagnetic field of up to 40° have been reported in young basalts drilled on the Mid-Atlantic Ridge (Ade-Hall et al., 1975b). Holes separated by only a few hundred meters have markedly different inclination profiles that could possibly be due to lava superimposition, the presence of separate small intrusions at differing ages, and tectonic tilting. In a study of basalts from 26 DSDP sites, Lowrie (1974) reported an average difference between remanent inclination and predicted geomagnetic field inclination of 14° and suggested that it is caused by secular variation. This is certainly a biasing factor in both trachytes and sediments from Holes 463 and 465A, because each sample spans less than 10,000 years, the period over which secular variation is averaged. Off-vertical drilling also imparts an error to inclination data. No dipmeter measurements were made at Hole 463, but Hole 465A is 4° out of the vertical at Core 40. Thus, a direct calculation of paleolatitudes from paleomagnetic inclinations is subject to a number of assumptions, not all of which can be satisfactorily tested, and although they can provide useful information, those paleolatitudes do not always provide a reliable absolute framework in which to test models of plate motion.

Two units drilled during Leg 62 that lend themselves to paleolatitude estimates are the Aptian–Albian multicolored and tuffaceous and carbonaceous limestones at Hole 463, and Units 3, 4, and 5 of the trachyte sequence at Hole 465A. They both carry a strong and well-defined direction of stable magnetization, with consistent inclination values throughout. Table 4 lists average inclinations and paleolatitude estimates for both these sequences. Note that it was not possible to determine the polarity of the Hole 465A trachytes, as discussed in the previous section, and that estimated paleolatitudes could be north or south of the equator.

Only a few models for Pacific Plate motion extend into the Cretaceous. The Lancelot model (Lancelot and Larson, 1974; Lancelot, 1978) is based on an analysis of sedimentary facies in deep-sea drill sites, Pacific Plate acoustic stratigraphy, and hot-spot trends. Epp (1979) has produced a model which is based purely on hot-spot trends and ages. They are similar in that both assume that major Pacific hot spots have been fixed relative to the earth's spin axis for the last 120 m.y., following the ideas of Morgan (1971). This assumption has been questioned by other authors (e.g., Burke et al., 1973; Molnar and Atwater, 1973; Molnar and Francheteau, 1975).

In addition, Hammond et al. (1979) point out that the Lancelot model differs from other models for Pacific Plate motion in the Cenozoic, among which there is good agreement. They also present paleomagnetic data from sediment cores from the central Pacific which disagree with all models. However flawed, it is interesting to compare these models with the Leg 62 paleomagnetic data (Tables 4 and 5). Results from both the limestones and trachytes show better agreement with the Lancelot model. Limestone inclinations are on the average about 10° shallower than that predicted by the Lancelot model, and approximately

Table 4. Average inclination (and standard deviations) and paleolatitude estimates from Hole 463 limestones and Hole 465A trachytes.

Hole	Cores	n	Mean Inclination (after demag.)	Est. Paleolatitude
463	55–71	67	$-27.1 \pm 9.8°$	8.9–20.6°S
465A	44–46	15	$\pm 7.5 \pm 4.7°$	1.4–6.2°N or S

Table 5. Paleolatitudes of Sites 463 and 465 during the Aptian and Albian, predicted by the Lancelot (1978) and Epp (1979) models of Pacific Plate motion.

Units	Age (m.y.)	Predicted Paleolatitude	
		Lancelot	Epp
Limestones	106–113.5	19.4–22.5°S	23.6–26.8°S
Trachytes	101?	3.8°S	7.9°S

16° shallower than predicted by the Epp model. This shallowing could be due to model error, or to any of the other factors discussed above.

There is good agreement between the trachyte results and the Lancelot model, if it is assumed that the trachytes were formed south of the equator. Thus, the predominance of negative inclinations in the trachyte sequence may reflect the predominance of normal polarity in the Albian.

ACKNOWLEDGMENTS

I would like to thank Drs. E. A. Hailwood and D. H. Tarling for their critical reviews and helpful comments on the manuscript. I am grateful to Adrian Manighetti for useful discussions on the trachyte results, Hilary Townsend for computer programming, Trisha Badham for drafting the figures, and Jane Windom for typing the final draft of the manuscript. I am eternally grateful to Mike Lehman and the Scripps technicians who were instrumental in keeping the shipboard magnetometer operating. Thanks also go to the co-chief scientists and the scientific crew of Leg 62 for close cooperation and stimulating discussion during the cruise. Financial support came from the Natural Environment Research Council.

REFERENCES

Ade-Hall, J. M., Johnson, H. P., and Ryall, P. J. C., 1975a. Rock magnetism of basalts, Leg 34. *In* Yeats, R. S., Hart, S. R., et al., *Init. Repts. DSDP*, 34: Washington (U.S. Govt. Printing Office), 459–468.

________, 1975b. Sources of magnetic anomalies on the Mid-Atlantic Ridge. *Nature*, 255:389–390.

Burke, K., Kidd, W. S. F., and Wilson, J. T., 1973. Relative and latitudinal motion of Atlantic hot spots. *Nature*, 245:133–137.

Cox, A., 1975. The frequency of geomagnetic reversals and the symmetry of the non-dipole field. *Rev. Geophys. Space Phys.*, 13: 35–51.

Epp, D., 1979. Pacific plate motion from hot spot traces. *Trans. Am. Geophys. Union*, 60:392.

Geological Society of London, 1964. Geological Society Phanerozoic time scale 1964. *Geol. Soc. London Quart. J.*, 120:260–262.

Green, K. A., and Brecher, A., 1974. Preliminary paleomagnetic results for sediments from Site 263, Leg 27. *In* Heirtzler, J., Veevers, J., et al., *Init. Repts. DSDP*, 27: Washington (U.S. Govt. Printing Office), 405–413.

Griffiths, D. H., King, R. F., Rees, A. I., et al., 1960. The remanent magnetism of some recent varved sediments. *Proc. Royal. Soc.* (ser. A), 256:359–383.

Grommé, C. S., Wright, T. L., and Peck, D. L., 1969. Magnetic properties and oxidation of iron-titanium oxide minerals in Alae and Makaopuhi lava lakes, Hawaii. *J. Gephys. Res.*, 74: 5277–5293.

Hailwood, E. A., 1977. Configuration of the geomagnetic field in early Tertiary times. *J. Geol. Soc.*, 133:23–26.

Hailwood, E. A., Bock, W., Costa, L., et al., 1979. Chronology and biostratigraphy of northeast Atlantic sediments, DSDP Leg 48. *In* Montadert, L., Roberts, D. G., et al., *Init. Repts. DSDP*, 48: Washington (U.S. Govt. Printing Office), 1119–1141.

Hailwood, E. A., Hamilton, N., and Morgan, G. E., 1980. Magnetic polarity dating of tectonic events at passive continental margins, *Phil. Trans. Royal Soc. London* (ser. A), 294:189–208.

Hammond, S. R., Epp, D., and Theyer, F., 1979. Neogene relative motion between the Pacific plate, the mantle, and the Earth's spin axis. *Nature*, 278:309–312.

Heirtzler, J. R., Dickinson, G. O., Herron, E. M., et al., 1968. Marine magnetic anomalies, geomagnetic field reversals, and motions of the ocean floor and continents, *J. Geophys. Res.*, 73:2119–2136.

Jarrard, R. D., 1974. Paleomagnetism of some Leg 27 sediment cores. *In* Heirtzler, J., Veevers, J., et al., *Init. Repts. DSDP*, 27: Washington (U.S. Govt. Printing Office), 415–423.

Johnson, H. P., and Merril, R. T., 1973. Low-temperature oxidation of a titanomagnetite and the implications for paleomagnetism. *J. Geophys. Res.*, 78:4938–4949.

Keating, B. H., and Helsley, C. E., 1978a. Paleomagnetic results from DSDP Hole 391C and the magnetostratigraphy of Cretaceous sediments from the Atlantic ocean floor. *In* Benson, W. E., Sheridan, R. E., et al., *Init. Repts. DSDP*, 44: Washington (U.S. Govt. Printing Office), 523–528.

________, 1978b. Magnetostratigraphy of Cretaceous age sediments from Sites 361, 363, and 364. *In* Bolli, H. M., Ryan, W. B. F., et al., *Init. Repts. DSDP*, 40: Washington (U.S. Govt. Printing Office), 459–468.

________, 1978c. Magnetostratigraphic studies of Cretaceous sediments from DSDP Site 369. *In* Lancelot, Y., Seibold, E., et al., *Init. Repts. DSDP*, Suppl. to Vols. 38, 39, 40, and 41: Washington (U.S. Govt. Printing Office), 983–986.

________, 1979. Cretaceous magnetostratigraphy. *Trans. Am. Geophys. Union*, 60:112.

Keen, M. J., 1963. The magnetization of sediment cores from the eastern basin of the North Atlantic Ocean. *Deep Sea Res.*, 10:607–622.

King, R. F., 1955. The remanent magnetism of artificially deposited sediments. *Monthly Notices Royal Astron. Soc., Geophys. Suppl.*, 7:115–134.

Lancelot, Y., 1978. Relations entre evolution sedimentaire et tectonique de la plaque pacifique depuis la Cretace Inferieur. *Mem. Soc. Geol. France*, 134.

Lancelot, Y., and Larson, R. L., 1974. Sedimentary and tectonic evolution of the northwestern Pacific. *In* Larson, R. L., Moberly, R., et al., *Init. Repts. DSDP*, 32: Washington (U.S. Govt. Printing Office), 925–939.

Larson, E., Ozima, M., Ozima, M., et al., 1969. Stability of remanent magnetization of igneous rocks. *Geophys. J. Royal Astron. Soc.*, 17:263–292.

Larson, R. L., and Hilde, T. W. C., 1975. A revised time scale of magnetic reversals for the Early Cretaceous and Late Jurassic. *J. Geophys. Res.*, 80:2586–2594.

Løvlie, R., 1974. Post-depositional rotational magnetization in a redeposited deep-sea sediment. *Earth Planet. Sci. Lett.*, 21:315–320.

________, 1976. The intensity pattern of post-deposition rotational magnetization acquired in some marine sediments deposited during a reversal of the external magnetic field. *Earth Planet. Sci. Lett.*, 30:209–214.

Lowrie, W., 1974. Oceanic basalt magnetic properties and the Vine and Matthews hypothesis. *J. Geophys.*, 40:513–536.

Lowrie, W., Alvarez, W., Premoli Silva, I., et al., 1979. Magnetic stratigraphy in Lower Cretaceous pelagic carbonate rocks from Umbria, Italy. *Trans. Am. Geophys. Union*, 60:112.

McElhinny, M. W., 1973. *Palaeomagnetism and Plate Tectonics:* Cambridge (Cambridge Univ. Press).

Marshall, M., 1978. The magnetic properties of some DSDP basalts from the North Pacific and inferences for Pacific plate tectonics. *J. Geophys. Res.*, 83:289–308.

Molnar, P., and Atwater, T., 1973. Relative motion of hot spots in the mantle. *Nature*, 246:288–291.

Molnar, P., and Francheteau, J., 1975. The relative motion of "hot spots" in the Atlantic and Indian oceans during the Cenozoic. *Geophys. J. Royal Astron. Soc.*, 43:763–744.

Morgan, W. J., 1971. Convection plumes in the lower mantle. *Nature*, 230:42–43.

Nagata, T., 1961. *Rock Magnetism:* Tokyo (Maruzen Company Ltd.).

Ozima, M., and Ozima, M., 1971. Characteristic thermomagnetic curve in submarine basalts. *J. Geophys. Res.*, 76:2051–2056.

Readman, P. W., and O'Reilly, W., 1972. Magnetic properties of oxidized (cation-deficient) titanomagnetites. *J. Geomagnet. Geoelec.*, 24:69–90.

Sakamoto, N., Ince, P. I., and O'Reilly, W., 1968. The effects of wet grinding on the oxidation of titanomagnetites. *Geophys. J. Royal Astron. Soc.*, 15:509–515.

van Hinte, J. E., 1976. A Cretaceous time scale. *Bull. Am. Assoc. Petrol. Geol.*, 60:498–516.

Wilson, R. L., 1970. Permanent aspects of the Earth's non-dipole magnetic field over upper Tertiary times. *Geophys. J. Royal Astron. Soc.*, 19:417–438.